Available online at www.pelagiaresearchlibrary.com

Pelagia Research Library

Advances in Applied Science Research, 2013, 4(4):465-478

ISSN: 0976-8610
CODEN (USA): AASRFC

The effect of hygroscopic growth on desert aerosols

B. I. Tijjani[1] and S. Uba[2]

[1]Department of Physics, Bayero University, Kano., Nigeria
[2]Department of Physics, Ahmadu Bello University, Zaria, Nigeria

---

ABSTRACT

In this paper some microphysical and optical properties of desertaerosolswereextracted from OPAC to determine the effect of hygroscopic growth at the spectral range of 0.25μm to 2.5μm and eight relative humidities (RHs) (0, 50, 70, 80, 90, 95, 98, and 99%). The microphysical properties extracted were radii, volume mix ratio, number mix ratio and mass mix ratio as a function of RH while the optical properties are scattering and absorption coefficients and asymmetric parameters. Using the microphysical properties, growth factors of the mixtures were determined while using optical properties we determined the enhancement parameters and were then parameterized using some models. We observed that the data fitted the models very well.

Keywords: microphysical properties, optical properties, hygroscopic growth, growth factors, enhancement parameters.

INTRODUCTION

Atmospheric aerosols are complex in their sources, evolutions, and interactions with water vapor in the atmosphere and as a result of that they affect the regional and global climate by participating in various atmospheric processes. Their hygroscopic response with the changes in relative humidity (RH) is critically important for their cloud condensation nuclei (CCN) activity, atmospheric residence time, optical property, microphysical property and chemical reactivity and so is one of the key factors in defining their impacts on climate. Atmospheric aerosol particles change in size due to water uptake which is determined by their chemical composition and the ambient relative humidity (RH). The effects of hygroscopic growth on optical properties are that primarily, it causes increase of the geometric sizes of the aerosol particles with increasing RH, and secondarily the decrease in the index of refraction of those particles that are solution drops with increasing RH as the drops become larger and thus more dilute.

It is well known however that absorption of water on insoluble particles (especially clays) can lead to hygroscopic growth similar to deliquescent salts (e.g., Schuttlefield et. al., 2007). This shows that the relative importance of the humidity dependences of particle size and index of refraction on the aerosol scattering coefficient for a given substance depends on RH and on the sizes of the particles that provide the dominant contribution to the scattering. The size and the solubility of a particle determine the response of an ambient particle to changes in RH. The water vapor pressure above a water droplet containing dissolved material is lowered by the Raoult effect. The equilibrium size of a droplet was first described by Kohler(1936), who considered the Kelvin (curvature) and Raoult (solute) effect. Past studies have demonstrated that calcite ($CaCO_3$) (a mineral with very low solubility compared to deliquescent salts) and Arizona Test Dust (ATD) can interact with water vapor and adsorb multiple layers of water under subsaturated conditions (Gustafsson et. al ., 2005; Vlasenko et. al., 2005; Hatch et. al., 2008). This interaction implies that dust mixtures and individual minerals with hydrophilic insoluble surfaces can affect water activity of aerosol (especially when the solute fraction of particles is low) with largely ignored implications for predicted CCN activity.

The study of particle hygroscopicity has a primary role in climate monitoring and weather forecast. Hygroscopic properties of aerosols, their size distribution and composition may alter the Earth's radiative budget (Pahlow et. al., 2006; Wulfmeyer and Feingold, 2000). Model studies have demonstrated that relative humidity has a critical influence on aerosol climate forcing (Pilinis et. al., 1995). Numerous studies have investigated the relationship between aerosol scattering and relative humidity RH in terms of the hygroscopic growth factor gf(RH) using humidified nephelometers. These have been used for airborne or ground-based determination of the growth factor considering a '' dry'' RH over the range 20% – 40% and a ''wet'' RH up to 90% (e.g.,Covert et al., 1972; McInne s et al., 1998; Kotchenruther et al., 1999; Malm et al., 2003).

This paper uses data extracted from OPAC on desert dust-water interactions to examine the importance of including hygroscopic growth on mineral dust aerosol. The microphysical properties extracted are radii, number mass mix ratios, mass mix ratios, volume mix ratios and effective refractive indicies while the optical properties are scattering, and absorption coefficients and assymetric parameters. The microphysical properties were used to determine the hygroscopic growth of the mixtures, which were later modelled using one and two parameters to determine their relations with RHs. The optical properties were used to determine the types of particle size distributions and their dependance on RH, and enhencement parameters were also modelled using one and two parameters to determine their relations with the RHs and wavelengths.

MATERIALS AND METHODS

The models extracted from OPAC are given in table 1.

Table 1 Compositions of aerosol type (Hess et al., 1998)

Aerosol model type	Components	Concentration N_i (cm^{-3})
Desert	WASO	2,000.0
	MINM	269.5
	MIAM	30.5
	MICM	0.142
	Total	2,300.142

where : N_i is the mass concentration of the component, water soluble components (WASO, consists of scattering aerosols, that are hygroscopic in nature, such as sulfates and nitrates present in anthropogenic pollution),mineral nucleation mode (MINM), mineral accumulation mode(MIAM) and mineral coarse mode (MICM).

The main parameter used to characterize the hygroscopicity of the aerosol particles is the aerosol hygroscopic growth factor gf(RH), which indicates the relative increase in mobility diameter of particles due to water absorption at a certain RH and is defined as the ratio of the particle diameter at any RH to the particle diameter at RH=0 and RH is taken for seven values 50%, 70%, 80%, 90%, 95%, 98% and 99%. (Swietlicki et al. , 2008; Randles, et al., 2004):

$$gf(RH) = \frac{D(RH)}{D(RH=0)} \quad (1)$$

The gf(RH) can be subdivided into different classes with respect hygroscopicity. One classification is based on diameter growth factor by Liu et al (2011) and Swietlicki et al., (2008) as barely Hygroscopic (gf(RH) = 1.0–1.11), Less Hygroscopic (gf(RH) = 1.11–1.33), More Hygroscopic (gf(RH)= 1.33–1.85) and most hygroscopic growth (gf(RH)> 1.85).

Atmospheric particles of a defined dry size typically exhibit different growth factors. This is due to either external mixing of particles in an air sample or variable relative fractions of different compounds in individual particles (the latter here in after referred to as quasi-internally mixed). A mono-modal growth distribution without spread can only be expected in very clean and homogeneous air parcels. For further details on mixing states see e.g. Buzorius et al. (2002).

Most atmospheric aerosols are externally mixed with respect to hygroscopicity, and consist of more and less hygroscopic sub-fractions (Swietlicki et al., 2008). The ratio between these fractions as well as their content of soluble material determines the hygroscopic growth of the overall aerosol. Particle hygroscopicity may vary as a function of time, place, and particle size (McMurry and Stolzenburg, 1989; Cocker et al., 2001; Swietlicki et al., 2008).

Prediction of hygroscopic growth factors with Kohler theory requires detailed knowledge of particle composition as well as a thermodynamic model, which describes the concentration dependence of the water activity for such a mixture. The hygroscopic growth factor of a mixture, $gf_{mix}(RH)$, can be estimated from the growth factors of the individual components of the aerosol and their respective volume fractions, V_k, using the Zdanovskii-Stokes-Robinson relation (ZSR relation; Sjogren et al., 2007; Stokes and Robinson, 1966; Meyer et al., 2009; Stock et al., 2011):

$$gf_{mix}(RH) = (\sum_k V_k gf_k^3)^{1/3} \quad (2)$$

where the summation is performed over all compounds present in the particles. Solute-solute interactions are neglected in this model and volume additivity is also assumed. The model assumes spherical particles, ideal mixing (i.e. no volume change upon mixing) and independent water uptake of the organic and inorganic components.

It can also be computed using the corresponding number fractions n_k as (Duplissy et al., 2011;Meier et al., 2009);

$$gf_{mix}(RH) = (\sum_k n_k gf_k^3)^{1/3} \quad (3)$$

Where n_k is the number fraction of particles having the growth factor gf_k .

We now proposed the $gf_{mix}(RH)$ to be a function of mass mix ratio as

$$gf_{mix}(RH) = (\sum_k m_k gf_k^3)^{1/3} \quad (4)$$

where the subscript k represents the different substances.

The RH dependence of $gf_{mix}(RH)$ can be parameterized in a good approximation by a one-parameter equation, proposed e.g. by Petters and Kreidenweis(2007):

$$gf_{mix}(a_w) = \left(1 + \kappa \frac{a_w}{1-a_w}\right)^{\frac{1}{3}} \quad (5)$$

Here, a_w is the water activity, which can be replaced by the relative humidity RH, if the Kelvin effect is negligible, as for particles with sizes more relevant for light scattering and absorption. At equilibrium, it can be shown that, over a flat surface, the water activity equals the ambient relative humidity in the sub-saturated humid environment (Seinfeld and Pandis, 1998; 2006). The coefficient κ is a simple measure of the particle's hygroscopicity and captures all solute properties (Raoult effect).

Humidograms of the ambient aerosols obtained in various atmospheric conditions showed that $gf_{mix}(RH)$ could as well be fitted well with a γ-law (Swietlicki et al., 2000; Birmili et al., 2004; Kasten, 1969; Gysel et al., 2009; Putaud, 2012) as

$$gf_{mix}(RH) = \left(1 - \frac{RH}{100}\right)^{\gamma} \quad (6)$$

Particle hygroscopicity is a measure that scales the volume of water associated with a unit volume of dry particle (Petters and Kreidenweis, 2007) and depends on the molar volume and the activity coefficients of the dissolved compounds (Christensen and Petters, 2012).

The bulk hygroscopicity factor B, which can be describe as the rate of obsorption of water with the increase in RH under subsaturation RH conditions was determined using the relation:

$$B = (1 - gf_{mix}^3) ln a_w \quad (7)$$

where a_w is the water activity, which can be replaced by the RH as explained before.

The impact of hygroscopic growth on the aerosol optical properties is usually described by the enhancement factor $f_\chi(RH,\lambda)$:

$$f_\chi(RH,\lambda) = \frac{\chi(RH,\lambda)}{\chi(RH=0,\lambda)} \quad (8)$$

where f_χ(RH,λ) can be denoting the aerosol scatteringand absorption coefficients, and asymmetry parameters. RH corresponds to any condition, and can cover the entire RH spectrum. In this paper we will only use scattering, absorption and asymmetric parameter. The reason for using asymmetric parameter is to determine the effect of hygroscopic growth on forward scattering. This method was initially introducedby Covert et al. (1972)

In general the relationship between $f_\chi(RH,\lambda)$ and RH is nonlinear (e.g. Jeong et al. 2007). In this paper we determine the empirical relations between the enhancement parameter and RH (Doherty et. al., 2005) as:

$$f_\chi(RH,\lambda) = \frac{\chi(RH,\lambda)}{\chi(RH=0,\lambda)} = \left(\frac{100-RH_{ref}}{100-RH_{high}}\right)^\gamma \quad (9)$$

where in our study RH_{ref} is 0%. The γknown as the humidification factor represents the dependence of aerosol optical propertiies on RH, which results from changes in the particle size and refractive index upon humidification. The parameter in our case was obtained by combining the eight $\chi(RH,\lambda)$parameters at 00%, 50%, 70%, 80%, 90%, 95%, 98% and 99% RH. The use of γhas the advantage of describing the hygroscopic behavior of aerosols in a non-linear manner over a broad range of RH values; it also implies that particles are deliquesced (Quinn et al. , 2005), a reasonable assumption for this data set due to the high ambient relative humidity during the field study. The γ parameter is dimensionless, and it increases with increasing particle water uptake. From previous studies, typical values of γ for ambient aerosol ranged between 0.1 and 1.5 (Gasso´ et. al., 2000; Quinn et al., 2005; Clarke et al., 2007).

Two parmeters empirical relation is also used (Jeong etal. 2007; Hanel (1976)) as;

$$f_\chi(RH,\lambda) = a\left(1-\frac{RH(\%)}{100}\right)^b \quad (10)$$

The model assumes equilibrium (metastable) growth of the aerosol scattering with RH such that the humidigraph profile does not display a deliquescent growth profile. For aerosol in a humid environment, this behavior will hold true. Most aerosols are a mixture of metastable and deliquescent particles and will exhibit some deliquescent behavior. We decided to validate models (9) and (10) at λ=0.25µm, λ=1.25µm and λ=2.50µm.

The Angstrom exponent being an indicator of the aerosol spectral behaviour of aerosols (Latha and Badarinath, 2005), the spectral behavior of the aerosol optical parameter (X, say), with the wavelength of light (λ) is expressed as inverse power law (Angstrom, 1961):

$$X(\lambda)=\beta\lambda^{-\alpha} \quad (11)$$

whereX(λ) can represent scattering and absorption coefficients.The variable X(λ) can be characterized by the Angstron parameter, which is a coefficient of the following regression,

$$\ln X(\lambda) = -\alpha\ln(\lambda) + \ln\beta \quad (12)$$

however the Angstrom exponent itself varies with wavelength, and a more precise empirical relationship between aerosol extinction and wavelength is obtained with a 2nd-order polynomial (King and Byrne, 1976; Eck et al., 1999; Eck. et al., 2001a, b,; Kaufman, 1993;O'Neill et al., 2001a, 2003; Pedros et al, 2003; Kaskaoutis and Kambezidis, 2006; Schmid et al., 2003;Martinez-Lozano et al., 2001) as:

$$\ln X(\lambda)=\alpha_2(\ln\lambda)^2 + \alpha_1\ln\lambda + \ln\beta \quad (13)$$

and then we proposed the cubic

$$\ln X(\lambda)= \ln\beta + \alpha_1\ln\lambda + \alpha_2(\ln\lambda)^2+ \alpha_3(\ln\lambda)^3 \quad (14)$$

where X(λ) can be any of the optical parameter,β, α, α_1, α_2, α_3 are constants that are determined using regression analysis with SPSS16.0.

We also determine the effect of hygroscopic growth on the effective refractive indices of the three mixed aerosolsusing the following formula (Aspens, 1982):

$$\frac{\varepsilon_{eff}-\varepsilon_0}{\varepsilon_{eff}+2\varepsilon_0} = \sum_{i=1}^{3} f_i \frac{\varepsilon_i-\varepsilon_0}{\varepsilon_i+2\varepsilon_0} \quad (15)$$

where f_i and ε_i are the volume fraction and dielectric constant of the i^{th} component and ε_0 is the dielectric constant of the host material. For the case of Lorentz-Lorentz (Lorentz, 1880; Lorentz, 1880), the host material is taken to be vacuum, ε_0 =1.

RESULTS AND DISCUSSION

Table 2: the growth factor of the aerosols using number mix ratio (equation 3) and Bulk hygroscopicity factor (equation 7)

RH(%)	50	70	80	90	95	98	99
gf_{mix}(RH)	1.0250	1.0914	1.1150	1.1594	1.2091	1.2773	1.3242
Bulk Hygroscopicityfactor (B)	0.0532	0.1070	0.0862	0.0588	0.0394	0.0219	0.0133

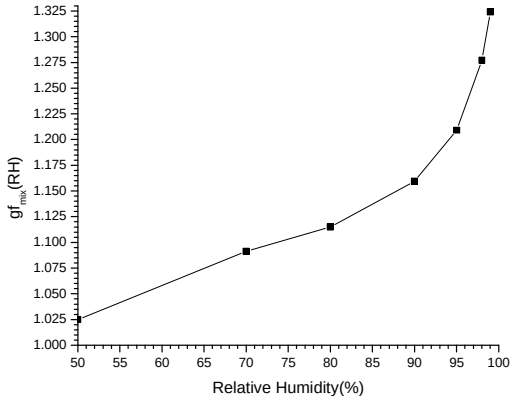

Figure 1; A graph of growth factor of the mixture using number mix ratio (equation 3)

Figure 1 shows a non-linear increase in hygroscopic growth with deliquescence as from 90 to 99%RH. The mixture can be described as less hygroscopic (Liu et. al., 2011; Swietlick et. al., 2008).

The results of the modelling using eqution (5) and (6) are given below:

C=1.3485, k=0.0112, R2=0.8364 (equation 5)

γ=-0.062512, R2=0.997060 (equation 6)

The fitted curve can be represented by one empirical parameters fit of the form of equations (5) and (6), though equation (6) has higher coefficient of determination.

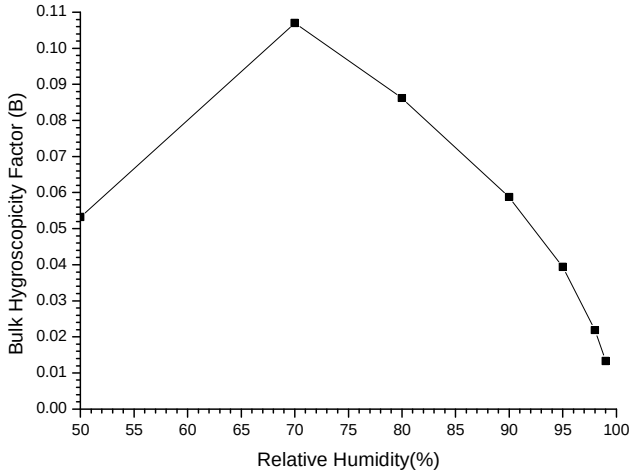

Figure 2; Bulk Hygroscopcity factor of the mixture using number mix ratio (equation 7)

Figure 2 shows that B increases almost linearly with RH from 50 to 70% RH. After 70% the graph dropped very sharply. This shows that the mixture absorbs more moisture as 50 to 70% while after that the rate of absorption decreases with the increase in RH. The nature of the plot from 70 to 99% shows the possibilities of internal mixing.

Table 3: the growth factor of the aerosols using volume mix ratio (equation 2) and Bulk hygroscopicity factor (equation 7)

RH(%)	50	70	80	90	95	98	99
gf_{mix}(RH)	1.0025	1.0046	1.0076	1.0150	1.0294	1.0643	1.1001
Bulk Hygroscopicityfactor (B)	0.0052	0.0050	0.0051	0.0048	0.0047	0.0042	0.0033

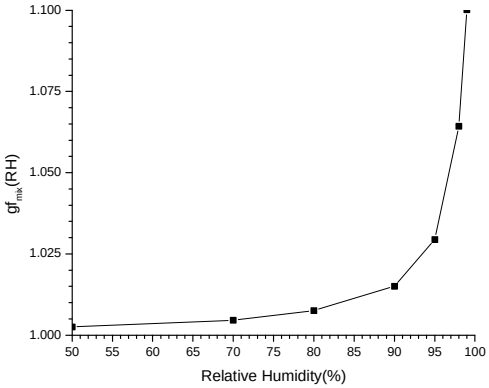

Figure 3, a graph of growth factor of the mixture using volume mix ratio (equation 2)

Figure 3is almost similar to figure 1 but the mixture can be described as barely hygroscopic.

The results of the modelling using eqution 5 and 6 are given below:

C=1.014828, k=0.003351, R2=0.985371 (equation 5)

γ=-0.014900, R2=0.868155 (equation 6)

The fitted curve can be represented by one empirical parameters fit of the form of equations (5) and (6), though equation (5) has higher coefficient of determination.

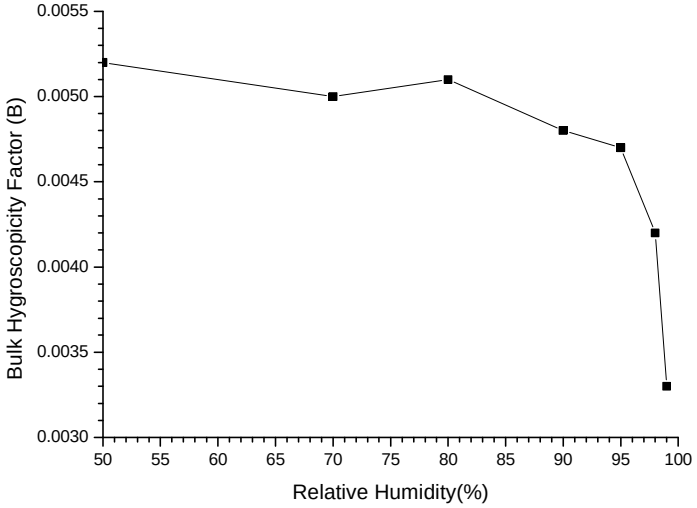

Figure 4; Bulk Hygroscopcity factor of the mixture using volume mix ratio (equation 7)

Figure 4 shows that between 50 and 95 % RH the mixture contained the mixtures of externally and internally mixed aerosols, because of the nature of the non-linearity of the plot. It also shows that 95 to 99%RH are the delequent points, because these are the points when the mixture is assumed to become internlly mixed.

Table 4: the growth factor of the aerosols using mass mix ratio (equation 4)and Bulk hygroscopicity factor (equation 7)

RH(%)	50	70	80	90	95	98	99
gf_{mix}(RH)	1.0013	1.0022	1.0040	1.0073	1.0138	1.0303	1.0488
Bulk Hygroscopicityfactor (B)	0.0028	0.0023	0.0027	0.0023	0.0021	0.0019	0.0015

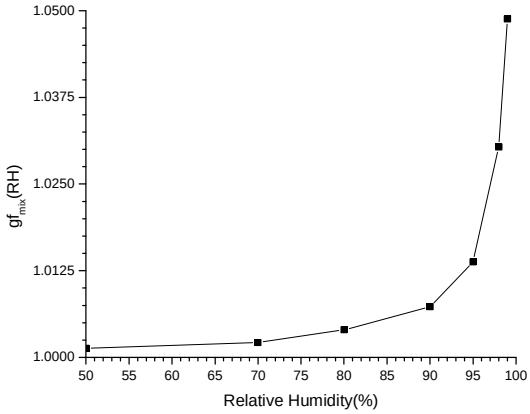

Figure 5; a graph of growth factor of the mixture using mass mix ratio (equation 4)

Figure 5is almost the same as figures 1 and 3. The mixture is barely hygroscopic.

The results of the modelling using eqution5 and 6 are given below:

C=1.007315, k=0.001542, R2=0.987689 (equation 5)

γ=-0.007306, R2=0.861313 (equation 6)

The fitted curve can be represented by one empirical parameters fit of the form of equations (5) and (6), though equation (5) has higher coefficient of determination.

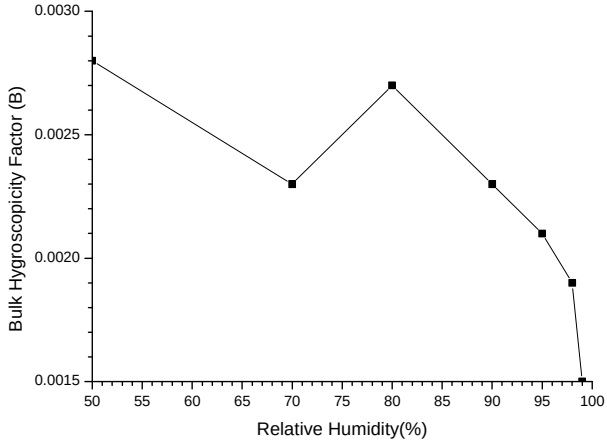

Figure 6; Bulk Hygroscopcity factor of the mixture using mass mix ratio (equation 7).

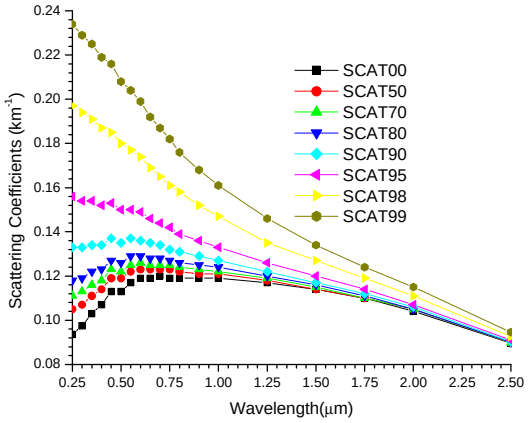

Figure 7: A plot of scattering coefficients against wavelength

Figure 6 shows that the plots at 50, 70 and 80% RH contained a mixture of externally and internally mixed aerosols and also the deliquent poing started from 90 to 99%.

Figure 7 shows the dominance of coarse particles, because of its nature at the small wavelenght, but it can be observed as the RH increases the hygroscopic growth has more effect on small particles because of the increase in scattering more at smaller wavelengths than at longer wavelengths. This increase is due to the growth of smaller particles to sizes at which they scatter more light being more pronounced than that for larger particles.

Table 5 The results of the Angstrom coefficients of scattering coefficients using equations (12), (13) and (14) for sahara model at the respective relative humidities using regression analysis with SPSS16.0

RH(%)	Linear		Quadratic			Cubic			
	R2	α	R2	α1	α2	R2	α1	α2	α3
0	0.0053	0.0101	0.9653	-0.0819	-0.2002	0.9829	-0.0515	-0.2349	-0.0455
50	0.0800	0.0355	0.9537	-0.1153	-0.1738	0.9805	-0.0812	-0.2127	-0.0510
70	0.2250	0.0606	0.9551	-0.1349	-0.1617	0.9817	-0.1002	-0.2012	-0.0518
80	0.3960	0.0853	0.9606	-0.1547	-0.1511	0.9839	-0.1203	-0.1903	-0.0515
90	0.6899	0.1389	0.9754	-0.1997	-0.1324	0.9890	-0.1673	-0.1694	-0.0485
95	0.8629	0.2082	0.9887	-0.2624	-0.1179	0.9937	-0.2362	-0.1478	-0.0392
98	0.9376	0.3124	0.9961	-0.3655	-0.1156	0.9967	-0.3522	-0.1307	-0.0198
99	0.9488	0.3841	0.9978	-0.4435	-0.1293	0.9978	-0.4399	-0.1335	-0.0055

Table 5 shows that in the linear part there is a poor correlation at RHs 0, 50, 70, and 80%. At RHs 90, 95, 98 and 99% RH the values of α reflects the dominance of coarse particles. At the quadratic part the sign of α2 which is being used to give more clarification of the type of particles failed. Probably may be because of the spectral range used. The cubic part gives some improvement over the correlations.

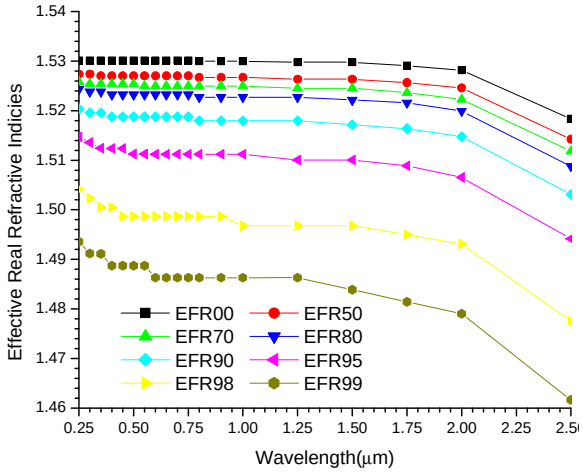

Figure 8: A plot of Effective real refractive indices against wavelengths

Figure 8 shows that hygroscopic growth has caused decreased in the effective real refractive indices. At 0% RH the plot is almost linear between 0.25μm to 2.0μm and this signifies spherical particles and at 2.0μm to 2.5μm shows the presence of non-spherical particles. The increase in RH decreases the effective refractive indices and the plots are becoming more non-linear with the increase in RHs. This shows that hygroscopic growth makes sphericla particles to become less spherical.

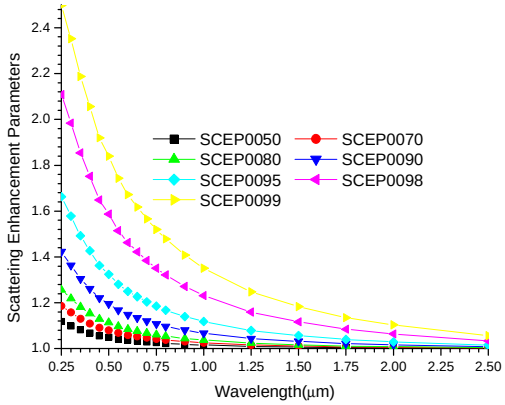

Figure 9: A plot of Scattering enhancement parameters against wavelengths

Figure 9 shows that the scattering enhancement is more noticeable at shorter wavelenghts and satisfies power law. This shows that hygroscopic growth has more effect on fine mode particles.

Enhancement factor as a function of RH shows a non linear relation. The results of the fitted curves of equations (9) and (10) are presented as follows:

For one parameter (equation 9)

At λ=0.25μ, γ=0.182958, R2=0.9900

At λ=1.25μ, γ=0.035933, R2=0.9000

At λ=2.50μ, γ=0.0083, R2=0.8600

For two parameters(equation 10)

At λ=0.25μ, a=0.917506, b=-0.209922, R^2=0.9860

At λ=1.25μ, a=0.947222, b=-0.052915, R^2=0.9139

At λ=2.50μ, a=0.985431, b=-0.012896,R^2=0.8813

From the values of R2 it can be observed that the data fitted our models very well.

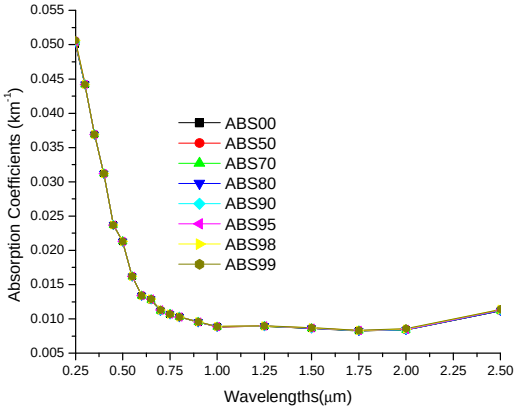

Figure 10: A plot of Absorption coefficients against wavelengths

Figure 10 shows that absorption is almost independent of RH and is higher at smaller wavelenghts. It also shows that it satisfies power law.

Table 6 The results of the Angstrom coefficients of absorption coefficients using equations (12), (13) and (14) for sahara model at the respective relative humidities using regression analysis with SPSS16.0

RH	Linear		Quadratic			Cubic			
(%)	R2	α	R2	α1	α2	R2	α1	α2	α3
0	0.7568	0.8058	0.9684	-0.5157	0.6315	0.9821	-0.6961	0.8374	0.2698
50	0.7562	0.8050	0.9686	-0.5144	0.6325	0.9821	-0.6932	0.8365	0.2673
70	0.7559	0.8047	0.9687	-0.5139	0.6329	0.9821	-0.6921	0.8362	0.2665
80	0.7557	0.8043	0.9688	-0.5134	0.6332	0.9822	-0.6912	0.8360	0.2659
90	0.7551	0.8036	0.9689	-0.5124	0.6340	0.9822	-0.6896	0.8361	0.2650
95	0.7541	0.8025	0.9690	-0.5108	0.6350	0.9822	-0.6875	0.8366	0.2643
98	0.7519	0.8003	0.9690	-0.5074	0.6375	0.9823	-0.6843	0.8392	0.2645
99	0.7497	0.7979	0.9689	-0.5040	0.6397	0.9824	-0.6816	0.8422	0.2655

The values of α from the linear part reflects the dominance of coarse particles together with R2. For the quadratic part, the sign of α2 also testifies this. The decrease in α and α1 also signifies the decrease in absorption with the increase in hygroscopic growth. The cubic shows some improvement over the R2, and this shows that the mixture can be bimodal

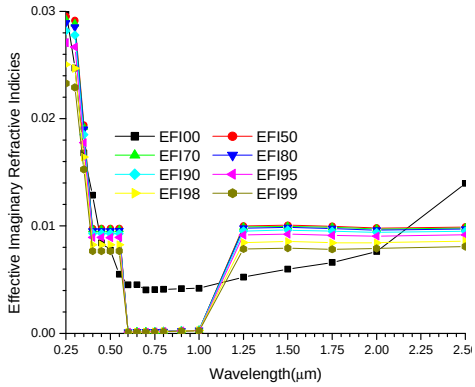

Figure 11: A plot of Effective Imaginary refractive indices against wavelengths

Figure 11 shows that hygroscopic growht has little effect on the imaginery part of refractive indices. At 0% RH the plots is non-linear and this probably happened because of the nature of the mixture. As the RH increase it can be observed that there is no definite relation between effective imaginary refractive indices and RH at this spectral range.

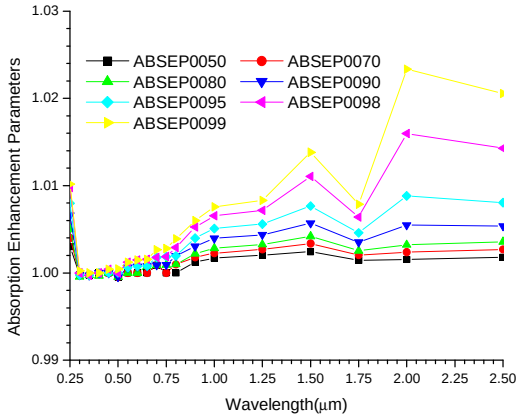

Figure 12: A plot of Absorption enhancement parameters against wavelengths

Figure 12 shows that the enhancement is very negligible at shorter wavelenghts and increases with the increase in wavelenghts.

Enhancement factor as a function of RH shows a non linear relation. The results of the fitted curves of equations (9) and (10) are presented as follows::

For one parameter (equation 9)

At λ=0.25μm, γ=0.002507, R2=0.980

At λ=1.25μm, γ=0.001856, R2=0.9950

At λ=2.50μm, γ=0.003538, R2=0.9500

For two parameters(equation 10)

At λ=0.25μ, a=1.001871, b=-0.001921, R^2=0.9843

At λ=1.25μ, a=1.000736, b=-0.001626, R^2=0.9984

At λ=2.50μ, a=0.996593, b=-0.004608, R^2=0.9290

All the models fit the data very well.

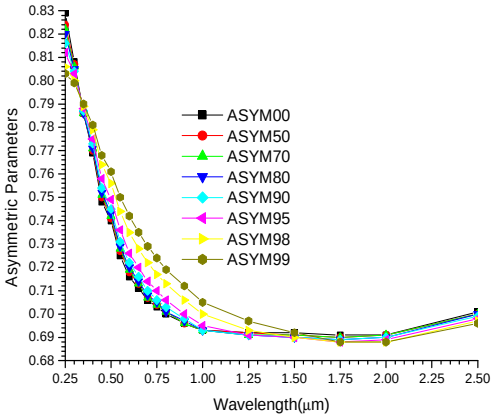

Figure 13 A plot of Asymmetric parameter against wavelength

Figure 13 shows that hygroscopic growth has less effect at shorter wavelengths but increases at wavelenghts 0.5 to 1.0 and decreases at shorter wavelengths. This shows that the increase in the hygroscopic growth enhences more scattering in the forward direction for small particles but enhences backward for big particles. This also shows the importance of the particle size in forward scattering.

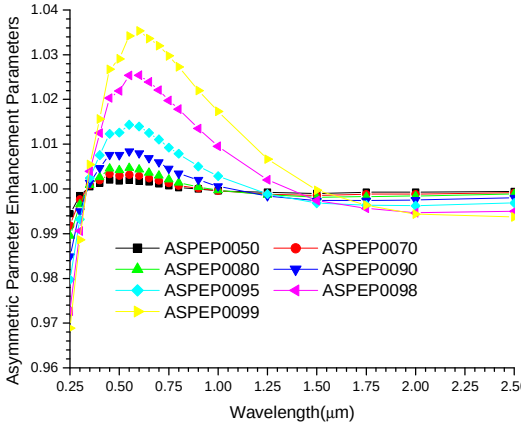

Figure 14: A plot of Asymmetric parameter enhancement parameters against wavelengths

Figure 14 shows that the enhancement factore is less than 1.0 at shorter wavelengths but started increasing as from 0.35 upto 1.0μm. As from 1.0μm it decreases upto where the enhencement becomes less that 1 and continued to decrease with the increase in wavelengths.

Enhancement factor as a function of RH shows a non linear relation. This shows that as the paricle size increases, there is a size that hygroscopic growth will cause the scattering to be equal in both forward and backward and as the size increases the scattering in the backward will also increase.The results of the fitted curves of equations (9) and (10) are presented as follows:

For one parameter (equation 9)

At λ=0.25μ, γ=-0.00689, R2=0.9990

At λ=0.55μ, γ=0.00592, R2=0.9380

At λ=1.25μ, γ=0.000494, R2=0.2400

At λ=2.50μ, γ=00119, R2=0.9690

The models fitted the data very well except at λ=1.25μm.

For two parameters (equation 10)

At λ=0.25μ, a=0.999993, b=0.006884, R^2=0.9968

At λ=0.55μ, a=0.992726, b=-0.008207, R2=0.9502

At λ=1.25μ, a=0.996303, b=-0.001654, R^2=0.6260

At λ=2.50μ, a=1.001026, b=0.001513, R^2=0.9708

The models fitted the data very well.

CONCLUSION

From the $gf_{mix}(RH)$ determined, it can be observed that despite the higher fractions of more strongly absorbing particles, very low values of $gf_{mix}(RH)$ were observed, and this is in line with what Sheridan et al. (2001) determined.

It shows that increase in hygroscopic growth increases forward scattering because particle growth enhances forward diffraction (Liou, 2002) for smaller particles while in larger particles it causes increase in the backward scattering, though the smallness has a limit as can be observed from assymmetric parameters and assymmetric enhancement parameters. It also shows that the mixture is internally mixed for smaller particles because of the increase in forward scattering as a result of the hygroscopic growth(Wang and Martin, 2007).

Finally, the data fitted our models very and can be used to extrapolate the hygroscopic growth at any RH and enhencement parameters at any RH and wavelength.

The modeling shows that hygroscopic growth at higher relative humidity increases the effective radii, scattering coefficients, scattering enhancement parameters, absorption coeffeicnts, absorption enhancement parameters, decreases effective real refractive indices but no definite relationship for effective imaginary refractive indices.

The nature of the effective real refractive indicies, assymmetric parameters and assymmetric enhancement parameters with the increase in RHs, shows that hygroscopic growth causes spherical particles to be less spherical and the less spherical to become more less spherical.

The more increase in scattering enhncement parameters at shorter wavelenghts and more increase in absorption enhancement parameters at longer wavelenghts shows that increase in hygroscopic growth causes increase in cooling for smaller particles while it causes increase in warming for bigger particles.

Finally it can be concluded that the importance of determining $gf_{mix}(RH)$ as a function of RH and volume fractions, mass fractions and number fractions, and enhancement parameters as a function of RH and wavelengths can be potentially important because it can be used for efficiently representing aerosols-water interactions in global models.

REFERENCES

[1] Angstrom, A.(**1961**): *Tellus*, 13, 214–223.
[2] Aspens D. E. (**1982**), *Am. J. Phys*. 50, 704-709.
[3] Birmili, W., Nowak, A., Schwirn, K., Lehmann, K.et al. (**2004**) *Journal of Aerosol Science* 1, 15–16, Abstracts of EAC, Budapest 2004.
[4] Buzorius, G., Zelenyuk, A., Brechtel, F., and Imre, D.: *Geophys. Res. Lett*., 29, **1974**, doi:10.1029/2001GL014221, 2002.
[5] Christensen, S. I. and Petters, M. D. (**2012**). *J. Phys. Chem*. A 116(39): 9706–9717.
[6] Clarke, A., et al. (**2007**), *J. Geophys. Res*., 11 2, D12S18, doi:10.1029/2006JD007777.
[7] Cocker, D., Whitlock, N., Flagan, R., and Seinfeld, J. H.: *Aerosol Sci. Technol*, 35, 2, 637–647, **2001**.
[8] Covert, D. S., R. J. Charlson, and N. C. Ahlquist (**1972**), *J. Appl. Meteor*., 11 , 968–976.
[9] Doherty, et al., **2005**. *Journal of Geophysical Research* 110, D04201.
[10] Duplissy J., P. F. DeCarlo, J. Dommen, M. R. Alfarra, A. Metzger, I. Barmpadimos, A. S. H. Prevot, E. Weingartner, T. Tritscher, M. Gysel, A. C. Aiken, J. L. Jimenez, M. R. Canagaratna , D. R. Worsnop, D. R. Collins, J. Tomlinson, and U. Baltensperger, (**2011**) *Chem. Phys*., 11, 1155–1165, www.atmos-chem-phys.net/11/1155/2011/ doi:10.5194/acp-11-1155-2011.
[11] Eck, T. F., Holben, B. N., Dubovic, O., Smirnov, A., Slutsker, I., Lobert, J. M., and Ramanathan, V.: Column-integrated aerosol optical properties over the Maldives during the northeast mon-soon for 1998–2000, J. *Geophys. Res*., 106, 28 555–28 566, **2001a**.

[12] Eck, T. F., Holben, B. N., Reid, J. S., Dubovic, O., Smirnov, A., O'Neil, N. T., Slutsker, I., and Kinne, S.: J. *Geophys. Res.*, 104(D24), 31 333–31 349, **1999**.
[13] Eck, T. F., Holben, B. N., Ward, D. E., Dubovic, O., Reid, J. S., Smirnov, A., Mukelabai, M. M., Hsu, N. C., O' Neil, N. T., and Slutsker, I.: *J. Geophys. Res*., 106(D4), 3425–3448, **2001b**.
[14] Gasso S., et al. (**2000**), *Tellus, Ser.* B , 52, 546 – 567.
[15] Gustafsson, R. J., A. Orlov, C. L. Badger, P. T. Griffiths, R. A. Cox, and R. M. Lambert (**2005**), *Atmos. Chem. Phys*., 5, 3415–3421.
[16] Gysel, M., McFiggans, G. B., and Coe, H.: *J. Aerosol Sci*., 40, 134–151, **2009**.
[17] Hanel, G. (**1976**). The Properties of Atmospheric Aerosol Particles as Functions of Relative Humidity at Thermodynamic Equilibrium with Surrounding Moist Air. InAdvances in Geophysics, Vol. 19 , H. E. Landsberg and J. Van Mieghem, eds., Academic Press, New York, pp. 73–188.
[18] Hatch, C. D., K. M. Gierlus, J. D. Schuttlefield, and V. H. Grassian (**2008**), *Atmos. Environ*., 42 , 5672-5684.
[19] Hess M., Koepke P., and Schult I (May **1998**), *Bulletin of the A merican Met. Soc*. 79, 5, p831-844.
[20] Jeong M. J, Li Z., Andrews E., Tsay S. C., (**2007**) Effect of aerosol humidification on the column aerosol optical thickness over the Atmospheric Radiation Measurement Southern Great Plains site, *J. Geophys. Res*., 112, D10202, doi:10.1029/2006JD007176.
[21] Kaskaoutis, D. G. and Kambezidis, H. D.(**2006**): *Q. J. R. Meteorol. Soc*., 132, 2217–2234,.
[22] Kasten, F.: Visibility forecast in the phase of pre-condensation, Tel-lus, XXI, 5, 631–635, **1969**.
[23] Kaufman, Y. J., *J. Geophys. Res*., 98, 2677-2992, **1993**.
[24] King, M. D. and Byrne, D. M.: *J. Atmos. Sci*., 33, 2242–2251, **1976**.
[25] Köhler, H. (**1936**), *Trans. Faraday Soc*., 32 (2), 1152-1161.
[26] Kohler, H.(**1936**): *Trans. Faraday Soc*., 32, 1152–1161.
[27] Kotchenruther, R. A., P. V. Hobbs, and D. A. Hegg (**1999**), *J. Geophys. Res.*, 104, 2239-2251.
[28] Latha, M.K., Badarinath, K.V.S., (**2005**). *Environmental Monitoring and Assessment* 104, 269–280.
[29] Liou, K. N. (2002), An Introduction ro Atmospheric Radiation, 583pp., Elsevier, New York.
[30] Liu P. F., Zhao C. S., Gobel T., Hallbauer E., Nowak A., Ran L., Xu W. Y., Deng Z. Z., Ma N., Mildenberger K., Henning S., Stratmann F., and Wiedensohler A. (**2011**) Hygroscopic proper ties of aerosol par ticles at high relative humidity and their diurnal variations in the Nor th China Plain, Atmos. Chem. Phys. Discuss., 11, 2991–3040
[31] Lorentz, H. A. (**1880**). *Ann. P hys. Chem*. 9, 641–665.
[32] Lorenz, L. (**1880**). *Ann. P hys. Chem*. 11, 70–103.
[33] Malm, W. C., D. E. Day, S. M. Kreidenwei s, J. L. Collett , and T. Lee (**2003**), *J. Geophys. Res.* , 108(D9), 4279, doi:10.1029/2002JD002998.
[34] Martinez-Lozano, J.A., Utrillas, M.P., Tena, F., Pedros, R., Canada, J., Bosca, J.V., Lorente, J., (**2001**). *IEEE Transactions on Geoscience and Remote Sensing* 39, 1573–1585.
[35] McInnes, L., M. Bergin, J. Ogren, and S. Schwartz (**1998**), *Geophys. Res. Lett*., 25, 4, 513-516.
[36] McMurry, P. and Stolzenburg, M.: *Atmos. Environ*., 23, 497–507, **1989**.
[37] Meier J., B. Wehner, A. Massling, W. Birmili, A. Nowak, T. Gnauk, E. Br¨ uggemann, H. Herrmann, H. Min, and A. Wiedensohler *Atmos. Chem. Phys*., 9, 6865–6880, **2009** www.atmos-chem-phys.net/9/6865/2009/
[38] Meyer, N. K., Duplissy, J., Gysel, M., Metzger, A., Dommen, J., Weingartner, E., Alfarra, M. R., Prevot, A. S. H., Fletcher, C., Good, N., McFiggans, G., Jonsson,˚ A. M., Hallquist, M., Baltensperger, U., and Ristovski, Z. D.: Analysis of the hy-groscopic and volatile properties of ammonium sulphate seeded and unseeded SOA particles, *Atmos. Chem. Phys*., 9, 721–732, doi:10.5194/acp-9-721-2009, **2009**.
[39] O'Neill, N. T., Dubovic, O., and Eck, T. F.(**2001**): *Appl. Opt*., 40(15), 2368–2375.
[40] O'Neill, N. T., Eck, T. F., Smirnov, A., Holben, B. N., and Thulasiraman, S.: Spectral dis-crimination of coarse and fine mode optical depth, *J. Geophys. Res*., 198(D17), 4559, doi:101029/2002JD002975, **2003**.
[41] Pahlow, M., Feingold, G., Jefferson, A., Andrews, E., Ogren, J.A., Wang, J., Lee, Y.-N., Ferrare, R.A., Turner, D.D. (**2006**). *J. Geophys. Res.* 111, D05S15. doi:10.1029/2004JD005646.
[42] Pedros, R., Martinez-Lozano, J. A., Utrillas, M. P., Gomez-Amo, J. L., and Tena, F.(**2003**): *J. Geophys. Res*., 108(D18), 4571, doi:10.1029/2002JD003331.
[43] Petters, M. D. and Kreidenweis, S. M. (**2007**). *Atmos. Chem. Phys.* 7(8): 1961–1971.
[44] Pilinis, C., Pandis, S.N., Seinfeld, J.H. (**1995**). *J. Geophys. Res.* 100, 18,739-18,754.
[45] Putaud, J.P.(**2012**): *Atmos. Chem. Phys. Discuss*., 12, C1316–C1322.
[46] Quinn, P. K., et al. (**2005**) , *Geophys. Res. Lett*., 32, L22809, doi:10.1029/2005GL024322.
[47] Randles , C. A. , Russell L. M. and. Ramaswamy V. (**2004**) *Geophysical Research Letters*, VOL. 31, L16108, doi:10.1029/2004GL020628.
[48] Schmid, B., Hegg, D.A., Wang, J., Bates, D., Redemann, J., Russell, P.B., Livingston, J.M., Jonsson, H.H., Welton, E.J., Seinfeld, J.H., Flagan, R.C., Covert, D.S., Dubovik, O., Jefferson, A., (**2003**). *Journal of Geophysical Research* 108 (D23), 8656.

[49] Schuttlefield, J. D., D. Cox, and V. H. Grassian (**2007**), An investigation of water uptake on clays minerals using ATR-FTIR spectroscopy coupled with quartz crystal microbalance measurements, *J. Geophys. Res*., 112, D21303, doi:10.1029/2007JD008973.
[50] Seinfeld, J. and Pandis, S. N.(**2006**): Atmospheric Chemistry and Physics, Wiley-Interscience, New York, NY, USA, 2nd edn.
[51] Seinfeld, J. H. and Pandis, S. N.(**1998**): Atmospheric Chemistry and Physics, Wiley-Interscience publication.
[52] Sheridan, P. J., D. J. Delene, and J. A. Ogren (**2001**), *J. Geophys. Res.* , 106 , 20,735 – 20,747.
[53] Sjogren, S., Gysel, M., Weingartner, E., Baltensperger, U., Cubi-son, M. J., Coe, H., Zardini, A. A., Marcolli, C., Krieger, U. K., and Peter, T.: *J. Aerosol Sci*., 38, 157–171, doi:10.1016/j.jaerosci.2006.11.005, **2007**.
[54] Stock M., Y. F. Cheng, W. Birmili, A. Massling, B. Wehner, T. Muller, S. Leinert, N. Kalivitis,N. Mihalopoulos, and A. Wiedensohler, *Atmos. Chem. Phys*., 11, 4251–4271, **2011** www.atmos-chem-phys.net/11/4251/2011/ doi:10.5194/acp-11-4251-2011
[55] Stokes, R. H. and Robinson, R. A.*: J. Phys. Chem*., 70, 2126–2130, **1966**.
[56] Swietlicki, E., Hansson, H.-C., H¨ameri, K., Svenningsson, B., Massling, A., et al.: Hygroscopic properties of submicrometer atmospheric aerosol particles measured with H-TDMA instru-ments in various environments – a review, *Tellus B*, 60(3), 432–469, **2008**.
[57] Swietlicki, E., Zhou, J., Covert, D. S., H¨ameri, K., Busch, B., V¨akeva, M., Dusek, U., Berg, O. H., Wiedensohler, A., Aalto, P., M¨akel¨a, J., Martinsson, B. G., Papaspiropoulos, G., Mentes, B., Frank, G., and Stratmann, F.: *Tellus*, 52B, 201–227, **2000**.
[58] Swietlicki, E.,et. al. (**2008**) *Tellus* B, 60, 432–469,.
[59] Vlasenko, A., S. Sjögren, E. Weingartner, H. W. Gäggeler, and M. Ammann (**2005**), *Aer. Sci. Tech*., 39 (5), 452-460.
[60] Wang, J., and S. T. Martin (**2007**), *J. Geophys. Res*., 112 , D 17203, doi:1 0.1029/2006JD008078.
[61] Wulfmeyer, V., Feingold, G. (**2000**). *J. Geophys. Res*. 105, 4729-4741.